

Free Energy Calculation from Steered Molecular Dynamics Simulations Using Jarzynski's Equality

Sanghyun Park,^{1,2} Fatemeh Khalili-Araghi,^{1,2} Emad Tajkhorshid,¹ and Klaus Schulten^{1,2}

¹Beckman Institute, University of Illinois at Urbana-Champaign, Urbana, Illinois 61801

²Department of Physics, University of Illinois at Urbana-Champaign, Urbana, Illinois 61801

(Dated: May 7, 2003)

Jarzynski's equality is applied to free energy calculations from steered molecular dynamics simulations of biomolecules. The helix-coil transition of deca-alanine in vacuum is used as an example. With about ten trajectories sampled, the second order cumulant expansion, among the various averaging schemes examined, yields the most accurate estimates. We compare umbrella sampling and the present method, and find that their efficiencies are comparable.

I. INTRODUCTION

Calculation of free energy is of great importance for understanding the kinetics and the structural determinants of biomolecular processes, such as transition between different conformations of DNA, folding and unfolding of proteins, ligand binding to receptors and enzymes, and transport of small molecules through channels. However, since they require thorough sampling of configuration space, free energy calculations are extremely costly for complex systems like biomolecules and efficient calculation of free energy is one of the most challenging tasks in computer simulations.¹ There exist various methods that are based on equilibrium or quasi-static simulations, such as thermodynamic integration² and umbrella sampling³ (for a review see Ref. 4). Triggered by the discovery of Jarzynski's equality,⁵ the realm of free energy calculation is now being extended to nonequilibrium simulations such as steered molecular dynamics (SMD). SMD simulations, reviewed in Refs. 6 and 7, have been widely used to investigate mechanical functions of proteins such as stretching⁷⁻¹⁰ or binding and unbinding.^{11,12} From the beginning SMD simulations have attempted to determine free energy profiles,^{13,14} and recently have employed Jarzynski's equality for that purpose.^{15,16}

Jarzynski's equality is a relation between *equilibrium* free energy differences and work done through *nonequilibrium* processes. Consider a process that changes a parameter λ of a system from λ_0 at time zero to λ_t at time t . The second law of thermodynamics states that the average work done on the system cannot be smaller than the difference between the free energies corresponding to the initial and the final values of λ :

$$\Delta F = F(\lambda_t) - F(\lambda_0) \leq \langle W \rangle, \quad (1)$$

where the equality holds only if the process is quasi-static (see e.g. Ref. 17). According to this inequality, a nonequilibrium process provides only an upper limit for the free energy difference. However, Jarzynski⁵ discovered an equality that holds regardless of the speed of the process:

$$e^{-\beta\Delta F} = \langle e^{-\beta W} \rangle. \quad (2)$$

This equality has been tested against computer simulations¹⁸ and experiments.¹⁹

Jarzynski's equality opens the possibility of calculating free energies from nonequilibrium processes. We refer to this approach as *nonequilibrium thermodynamic integration*, as opposed to the conventional thermodynamic integration based on quasi-static processes for which ΔF equals $\langle W \rangle$. Various nonequilibrium processes that are routinely studied in computer simulations or experiments (for example, stretching proteins or RNA, pulling a small molecule through a channel, etc.) can now be used for free energy calculations. Some work has been done in this regard,^{15,16,20-24} but free energy calculations from nonequilibrium processes as yet remain a challenge. The major difficulty is that the average of exponential work appearing in Jarzynski's equality is dominated by the trajectories corresponding to small work values that arise only rarely. An accurate estimate of free energy, hence, requires suitable sampling of such rare trajectories. Therefore, although Jarzynski's equality holds for processes of any speed, practical applications are currently limited to slow processes for which the fluctuation of work is comparable to the temperature.

The purpose of this paper is to guide the application of Jarzynski's equality to the calculation of free energies from SMD simulations, with the main focus on large systems such as biomolecules. In SMD simulations, one applies force to induce the process of interest so that one can focus on important aspects while minimizing the computational cost.^{6,7,25} Often, because of limited computing power, a process involving native biopolymers is simulated at a speed several orders of magnitude higher than the quasi-static speed, and besides one can sample only a small number of trajectories. Thus, Jarzynski's equality may not appear to be promising in this case. However, one can overcome this difficulty to a certain extent by using approximate formulas via the cumulant expansion.^{5,15,22}

We introduce a method of free energy calculations based on Jarzynski's equality. The helix-coil transition of deca-alanine, which is relevant to protein folding, is used as an exemplary system. The transition is induced by fixing one end of the molecule and pulling the other end. The free energy as a function of the end-to-end distance

is calculated with various averaging schemes, namely the exponential average [Eq. (2)] and various orders of the cumulant expansion. We examine the accuracy of the calculated free energies to find which averaging scheme works best at which pulling speed and how much error one would expect with a limited number of trajectories. We also perform umbrella sampling and compare its efficiency to that of the present method.

II. FREE ENERGY CALCULATION BASED ON JARZYNSKI'S EQUALITY AND THE STIFF-SPRING APPROXIMATION

In most cases, free energy calculations are aimed at *relative* free energies; one is interested in how free energy *changes* as a function of either an external parameter or an internal coordinate. In this section we describe a method of using Jarzynski's equality for calculating free energy with respect to an internal coordinate. A free energy profile as a function of a coordinate is called a potential of mean force (PMF), and the coordinate is referred to as the reaction coordinate.

Consider a classical mechanical system of N particles described by molecular dynamics simulation at constant temperature T . A state of the system is specified by $3N$ -dimensional position \mathbf{r} and momentum \mathbf{p} . Suppose that we are interested in the PMF $\Phi(\xi)$ of the system with respect to some reaction coordinate $\xi(\mathbf{r})$. The PMF $\Phi(\xi)$ is defined by

$$\exp[-\beta\Phi(\xi')] = \int d\mathbf{r} d\mathbf{p} \delta(\xi(\mathbf{r}) - \xi') \exp[-\beta H(\mathbf{r}, \mathbf{p})], \quad (3)$$

where β is the inverse temperature ($\beta = 1/k_B T$) and H is the Hamiltonian. In order to apply Jarzynski's equality to the calculation of $\Phi(\xi)$, we need to introduce an external parameter λ in such a way that λ is correlated with ξ . This can be achieved by adding a guiding potential

$$h(\mathbf{r}; \lambda) = \frac{k}{2} [\xi(\mathbf{r}) - \lambda]^2, \quad (4)$$

i.e. a spring, that constrains ξ to be near λ . The Hamiltonian of the new system (the original system plus the guiding potential) is then

$$\tilde{H}(\mathbf{r}, \mathbf{p}; \lambda) = H(\mathbf{r}, \mathbf{p}) + h(\mathbf{r}; \lambda). \quad (5)$$

The region of ξ for which the PMF $\Phi(\xi)$ is to be calculated is covered by changing λ with a constant velocity: $\lambda_t = \lambda_0 + vt$. This scheme of a moving guiding potential matches particularly well SMD simulations⁷ and atomic force microscope experiments.²⁶

By employing, for example, Nose-Hoover thermostat^{27,28} or Langevin dynamics schemes, constant-temperature molecular dynamics simulations can be implemented in a manner that satisfies the conditions for Jarzynski's equality, namely the Markov property and detailed balance.¹⁸ Applying Jarzynski's equality [Eq. (2)] to the \tilde{H} -system leads to

$$\exp\{-\beta[F(\lambda_t) - F(\lambda_0)]\} = \langle \exp(-\beta W_{0 \rightarrow t}) \rangle. \quad (6)$$

Here F is the Helmholtz free energy of the \tilde{H} -system,

$$\exp[-\beta F(\lambda)] = \int d\mathbf{r} d\mathbf{p} \exp[-\beta \tilde{H}(\mathbf{r}, \mathbf{p}; \lambda)], \quad (7)$$

and $W_{0 \rightarrow t}$ is the work done on the \tilde{H} -system during the time interval between zero and t ,

$$W_{0 \rightarrow t} = \int_0^t dt' \frac{\partial \lambda_{t'}}{\partial t'} \left[\frac{\partial \tilde{H}(\mathbf{r}, \mathbf{p}; \lambda)}{\partial \lambda} \right] (\mathbf{r}_{t'}, \mathbf{p}_{t'}; \lambda_{t'}) \quad (8)$$

Note that the work $W_{0 \rightarrow t}$ depends on an entire trajectory, not just its initial and final states. The average $\langle \cdot \rangle$ is taken over the ensemble of trajectories whose initial states $(\mathbf{r}_0, \mathbf{p}_0)$ are sampled from the canonical ensemble corresponding to the Hamiltonian $\tilde{H}(\mathbf{r}_0, \mathbf{p}_0; \lambda_0)$.

So far, we have obtained a formula for the free energy F of the \tilde{H} -system. But what we actually want is the PMF Φ of the original H -system. In general, since $\xi(\mathbf{r}_t)$ fluctuates among trajectories, in order to calculate $\Phi(\xi)$ one needs to combine the work $W_{0 \rightarrow t}$ for different values of t (or λ). This is not impossible (see Ref. 21), but an easier and perhaps more efficient way is to use a sufficiently large force constant k for the guiding potential, i.e. a sufficiently stiff spring, so that the reaction coordinate ξ closely follows the constraint center λ .

The free energy F can be written in terms of the PMF Φ as follows:

$$\begin{aligned} \exp[-\beta F(\lambda)] &= \int d\mathbf{r} d\mathbf{p} \exp \left\{ -\beta H(\mathbf{r}, \mathbf{p}) - \frac{\beta k}{2} [\xi(\mathbf{r}) - \lambda]^2 \right\} \\ &= \int d\mathbf{r} d\mathbf{p} \int d\xi' \delta(\xi(\mathbf{r}) - \xi') \exp \left\{ -\beta H(\mathbf{r}, \mathbf{p}) - \frac{\beta k}{2} [\xi(\mathbf{r}) - \lambda]^2 \right\} \\ &= \int d\xi' \exp \left[-\beta \Phi(\xi') - \frac{\beta k}{2} (\xi' - \lambda)^2 \right]. \end{aligned} \quad (9)$$

When k is large, most contribution to the preceding integral comes from the region around λ , which leads to the stiff-spring approximation:

$$F(\lambda) \approx \Phi(\lambda). \quad (10)$$

In Appendix, we systematically derive the stiff-spring approximation including the correction terms. Using this result in Eq. (6), we obtain

$$\Phi(\lambda_t) = \Phi(\lambda_0) - \frac{1}{\beta} \log \langle \exp(-\beta W_{0 \rightarrow t}) \rangle. \quad (11)$$

$$\log \langle e^{-\beta W} \rangle = -\beta \langle W \rangle + \frac{\beta^2}{2} (\langle W^2 \rangle - \langle W \rangle^2) - \frac{\beta^3}{3!} (\langle W^3 \rangle - 3\langle W^2 \rangle \langle W \rangle + 2\langle W \rangle^3) + \dots, \quad (12)$$

where the subscripts of W are suppressed. If the distribution of work W is Gaussian, third and higher cumulants are identically zero.²⁹ Depending on the number of terms being kept, various orders of approximation are possible. In fact, the second order cumulant expansion formula is identical to the near-equilibrium formula^{30,31} predating Jarzynski's equality. But only after the discovery of Jarzynski's equality, the near-equilibrium formula was recognized as an approximation to the exponential average.

When these approximate formulas are used, two kinds of error are involved: a systematic error due to the truncation of higher order terms and a statistical error due to insufficient sampling. If an infinite number of trajectories were available, the statistical error would vanish and hence the exponential average, Eq. (11), would give the best estimate for Φ ; there would be no need to use the cumulant expansion in this case. However, since in practice only a limited number of trajectories are sampled, the statistical error may dominate the systematic error. Thus, the approximate formulas may give better results since lower order cumulants are estimated with smaller statistical errors.

III. HELIX-COIL TRANSITION OF DECA-ALANINE: ACCURACY OF THE CALCULATED FREE ENERGY

In this section, we apply the method described above to an exemplary system, helix-coil transition of deca-alanine in vacuum, and examine the accuracy of the resulting free energy. Deca-alanine is an oligopeptide composed of ten alanine residues (Fig. 1). In vacuum at room temperature, the stable configuration of deca-alanine is an α -helix.³³ We confirmed this by several equilibrium simulations with various initial conformations including extended coil, α -helix, and β -hairpin. All the simula-

The exponential average $\langle \exp(-\beta W_{0 \rightarrow t}) \rangle$ is dominated by the trajectories corresponding to small $W_{0 \rightarrow t}$ values and, therefore, is difficult to estimate because such trajectories are rarely sampled. Approximate formulas provided by the cumulant expansion are often more effective.^{5,15,22} The last term in Eq. (11) can be expanded in terms of cumulants:

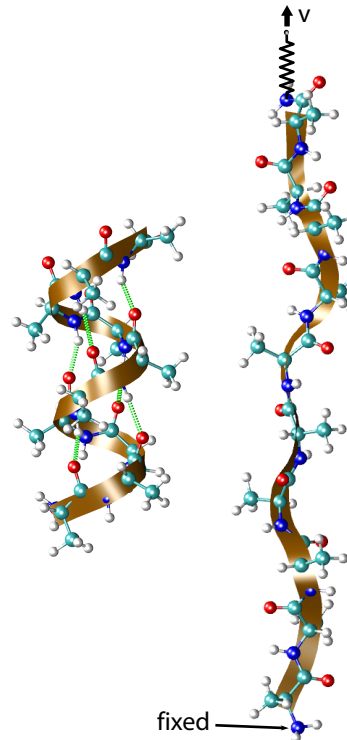


FIG. 1: Unfolding of helical deca-alanine. *Left*, a folded configuration (α -helix). The six hydrogen bonds that stabilize the helix are shown. *Right*, an extended configuration (coil). The backbone of the peptide is represented as a ribbon. The N atom of the first residue was fixed during the simulations. The moving guiding potential used in the pulling simulations is represented by a spring which is connected to the C-terminus and pulled with a constant velocity v . Figure made with VMD.³²

tions converged to the α -helix structure. Stretching the molecule by an external force can induce its transition to an extended form (coil). This helix-coil transition repre-

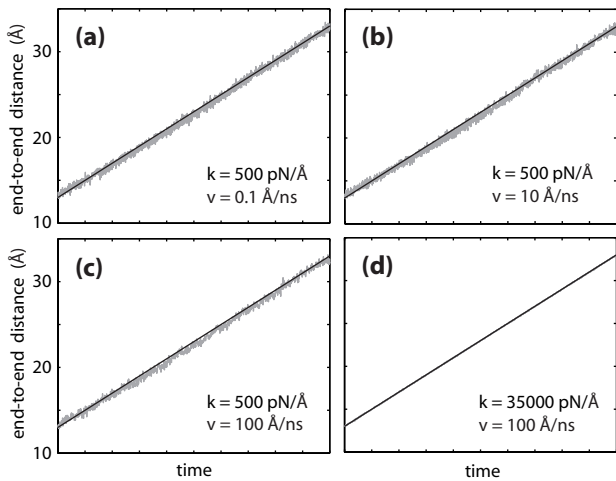


FIG. 2: Typical trajectories (end-to-end distance vs. time) for different values of the force constant k and the pulling velocity v . The horizontal axes (time) are appropriately scaled. The straight lines represent the position of the constraint center. In (d), the trajectory is indistinguishable from the straight line.

sents a simple but basic folding system, hence constituting an interesting problem. We calculate the PMF $\Phi(\xi)$ of the molecule with respect to the end-to-end distance ξ of the molecule.

Deca-alanine is chosen because it is suitable for a systematic study. The system is small enough (104 atoms) to permit simulation of many trajectories, yet complex enough to be considered a prototype of a large biopolymer. Also, since the system does not contain solvent molecules, the relaxation time is sufficiently short that the helix-coil transition can be induced in a reversible manner. The work done during the reversible simulation can be considered the exact free energy and be used for assessing the accuracy of the free energies calculated from irreversible (nonequilibrium) simulations.

In the simulation, we fix one end of the molecule (the N atom of the first residue) at the origin and constrain the other end (the capping N atom at the C-terminus) to move only along the z -axis, thereby removing the irrelevant degrees of freedom, i.e., overall translation and rotation.³⁴ A guiding potential $h(\mathbf{r}; \lambda) = (k/2)(\xi(\mathbf{r}) - \lambda)^2$ is added to control the end-to-end distance ξ . Obviously, ξ is a function of the $3N$ -dimensional position \mathbf{r} of the system. The parameter λ is changed between 13 Å and 33 Å with various constant velocities v . A force constant of $k = 500$ pN/Å is used, unless mentioned otherwise. With this force constant, the end-to-end distance ξ closely follows the constraint center λ as can be seen in Fig. 2. From Eq. (8), the external work is calculated as

$$W_{0 \rightarrow t} = -kv \int_0^t dt' (\xi(\mathbf{r}_{t'}) - \lambda_0 - vt'). \quad (13)$$

Depending on the sign of v , the procedure corresponds to either stretching or contracting the molecule. For

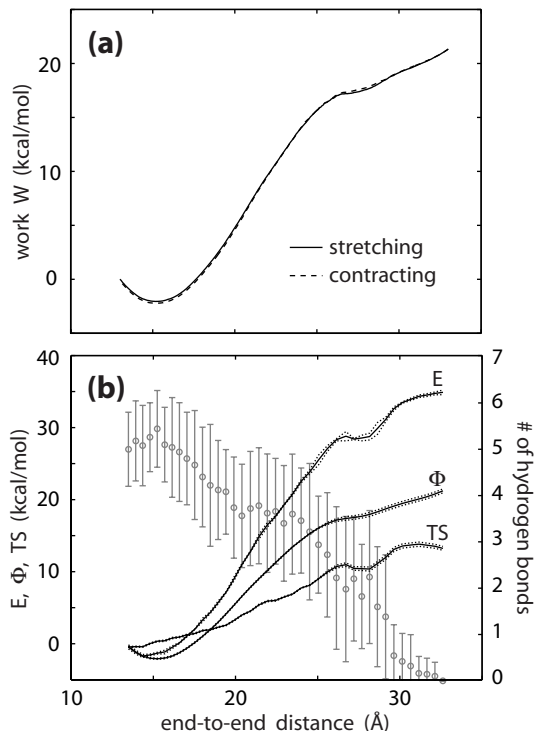


FIG. 3: Reversible pulling ($|v| = 0.1$ Å/ns). (a) Work done by forward pulling (stretching) and backward pulling (contracting). For the forward pulling, the position of the constraint center λ is varied from 13 to 33 Å; for the backward pulling, from 33 to 13 Å. For the sake of comparison, the backward-pulling work curve has been shifted vertically so that it coincides with the forward-pulling work curve at $\lambda = 33$ Å. (b) Energy E , PMF Φ , and entropy S calculated from four forward pullings. The error bars are shown as dotted lines. Also shown is the number of hydrogen bonds (averaged over time windows) plotted against the end-to-end distance (circles with error bars). A minimum heteroatomic distance of 3.5 Å (between N and O) and a minimum bond angle of 140° (N-H...O) were used for defining a hydrogen bond.

the sampling of trajectories, we select initial coordinates from an ensemble generated by a 1 ns equilibrium simulation with λ fixed at λ_0 , and initial momenta from the Maxwell-Boltzmann distribution. All simulations were done at constant temperature (300 K) with the temperature controlled by Langevin dynamics. We used the molecular dynamics program NAMD³⁵ with the CHARMM22 force field.³⁶

A. Reversible pulling

To induce the unfolding in a reversible manner, we tried stretching the molecule at various pulling speeds. For each pulling speed, the reverse event (contracting) was also simulated by applying the same speed in the opposite direction. We find that at a pulling speed of 0.1 Å/ns, which requires 200 ns of simulation for the full

extension, the process is reversible as can be seen from the overlap of the two work curves corresponding to forward pulling (stretching) and backward pulling (contracting) in Fig. 3a. Therefore, Eq. (1) becomes an equality in this case:

$$F(\lambda_t) - F(\lambda_0) = \langle W_{0 \rightarrow t} \rangle, \quad (14)$$

or, using the stiff-spring approximation [Eq. (10)],

$$\Phi(\lambda_t) = \Phi(\lambda_0) + \langle W_{0 \rightarrow t} \rangle. \quad (15)$$

From four repeated forward pulling simulations, we estimate $\langle W_{0 \rightarrow t} \rangle$, and obtain Φ ; the outcome is plotted in Fig. 3b. The standard deviation of the work W , shown as error bars in Fig. 3b, is small (less than $0.5 k_B T$) as expected in the reversible regime. The PMF calculated from these reversible pullings is considered exact and will be used as a reference for assessing the accuracy of the results obtained from irreversible pulling simulations.

Although the focus of the present study lies on methodology, it is worth noting some interesting features of the obtained free energy profile. The PMF assumes a minimum at $\xi \approx 15.2 \text{ \AA}$, corresponding to the helical structure of the molecule that forms in the absence of the constraint. Departing from this minimum, the free energy increases as the molecule is stretched into a coil. Free energy can be divided into energy and entropy:

$$\Phi(\xi) = E(\xi) - TS(\xi). \quad (16)$$

The energy E can be calculated from the Hamiltonian $H(\mathbf{r}, \mathbf{p})$. We first take averages over time windows of 5 ns to smooth out the fluctuation (of the order of \sqrt{N}) and then take averages over the four trajectories: $E(\lambda_t) = \langle H(\mathbf{r}_t, \mathbf{p}_t) \rangle$. The entropy S is then calculated from Eq. (16). As can be seen in Fig. 3b, the entropy generally increases with the end-to-end distance, reflecting that a larger configuration space is available to the coil than to the helix.³⁷ The energy also increases with ξ , but faster than the entropy, thereby making the free energy increase with ξ from the equilibrium distance 15.2 \AA . Most of the increase of the energy $E(\xi)$ can be attributed to the breaking of the intrahelical hydrogen bonds. Fig. 3b clearly shows that the number of hydrogen bonds decreases as the molecule is stretched.

B. Free energy calculation from irreversible pulling

In studying large systems like biomolecules, the time scale accessible to computer simulation is often much shorter than the natural time scale of the process of interest. Therefore, such a process needs to be accelerated in simulations; in addition, only a small number of trajectories (typically about ten) can be obtained. In order to study the helix-coil transition of deca-alanine in a comparable situation, we stretch the molecule at speeds higher than the speed of the reversible regime. It is then examined heuristically what accuracy one can achieve in the

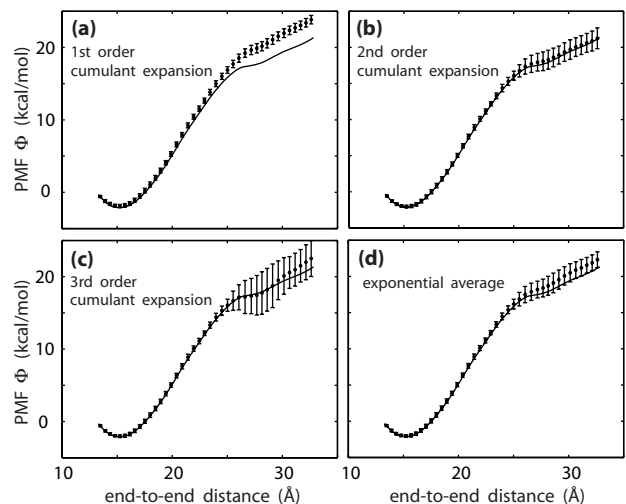


FIG. 4: PMF calculated from irreversible pulling ($v = 10 \text{ \AA/ns}$) through the block average of 10 blocks of 10 trajectories. The error bars indicate the standard deviation over the blocks. The exact PMF calculated from the reversible pulling is plotted as a solid line in each panel.

free energy calculation from a limited number of nonequilibrium trajectories and which averaging scheme gives the best result.

1. Comparing various averaging schemes

We use two different pulling speeds, $v = 10$ and 100 \AA/ns , for our irreversible simulations. These speeds are 100 and 1000 times higher than the speed used for the reversible regime. For each pulling speed, 100 trajectories were generated and grouped into 10 blocks of 10 trajectories. Figs. 4 and 5 show the averages and the standard deviations of the PMFs calculated from the blocks of 10 trajectories. Four different averaging schemes are tested: the exponential average [Eq. (11)] and the first, second, and third orders of the cumulant expansion [Eq. (12)].

Since the process is irreversible, the average external work done on the system (identical to the first order cumulant expansion) is larger than the free energy difference. The excess amount of work, known as the irreversible work, grows with the pulling distance. For $v = 10 \text{ \AA/ns}$, it grows up to 2.7 kcal/mol ($4.5 k_B T$). This irreversible work is discounted by Jarzynski's equality. As can be seen in Fig. 4, both the second order cumulant expansion and the exponential average yield reasonably good estimates for the free energy, though the former is slightly better than the latter. The third order cumulant expansion shows big fluctuations (over the blocks).

For $v = 100 \text{ \AA/ns}$, the irreversible work is much larger, growing up to 18.8 kcal/mol ($31.3 k_B T$). In this case, the second order cumulant expansion again gives the best estimate. The third order again shows big fluctuations. We have also examined fourth order results, but they

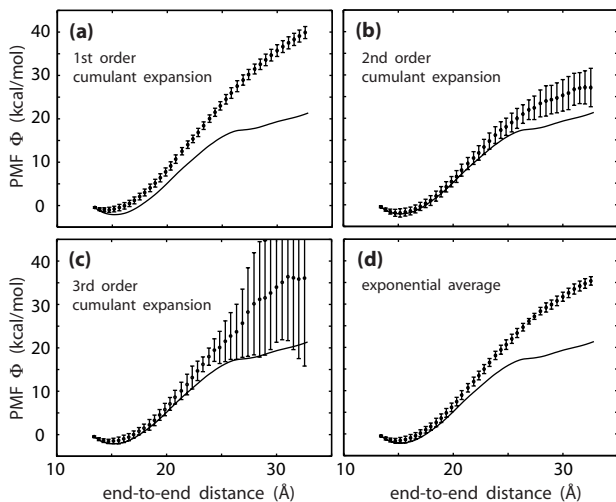


FIG. 5: PMF calculated from irreversible pulling ($v = 100 \text{ \AA/ns}$) through the block average of 10 blocks of 10 trajectories. The error bars indicate the standard deviation over the blocks. The exact PMF calculated from the reversible pulling is plotted as a solid line in each panel.

show even bigger fluctuations (not shown here). As for the exponential average, the fluctuation over the blocks is relatively small but the estimate is far from the actual PMF. This is due to the slow convergence of the exponential average, and suggests that *good statistics in block averaging do not always imply accurate estimates*. This can be explained roughly as follows. For an accurate estimate of the exponential average, $e^{-\beta\Delta F} = \langle e^{-\beta W} \rangle$, one

needs to sample work values around ΔF . With a limited number of trajectories, the region around ΔF may not be sampled at all. For $v = 100 \text{ \AA/ns}$, all the 100 total work values (for the full extension) fall within the region $35 \text{ kcal/mol} \lesssim W \lesssim 50 \text{ kcal/mol}$, while the free energy difference between the initial and final conformations is only 21.4 kcal/mol . This makes the exponential-average estimate far from the actual free energy difference. On the other hand, the function $e^{-\beta W}$ changes only by a small amount within the region where the 100 work values were sampled, which makes the variance of the exponential average small.

2. Finite-Sampling correction

With M independently sampled work values W_i , the free energy estimate given by the exponential average [Eq. (2)] is biased^{24,30} because

$$\left\langle -\frac{1}{\beta} \log \frac{1}{M} \sum_{i=1}^M e^{-\beta W_i} \right\rangle \geq -\frac{1}{\beta} \log \langle e^{-\beta W} \rangle = \Delta F, \quad (17)$$

where the equality holds if M is infinite. The inequality is due to the convexity of the logarithmic function. In general, any finite-sampling estimate of a nonlinear average is biased. The cumulant expansion [Eq. (12)] is not an exception. For the second order cumulant expansion which, according to our results, is the best choice for a small number of trajectories, the bias is expressed as

$$\left\langle \frac{1}{M} \sum_{i=1}^M W_i - \frac{\beta}{2} \left[\frac{1}{M} \sum_{i=1}^M W_i^2 - \left(\frac{1}{M} \sum_{i=1}^M W_i \right)^2 \right] \right\rangle \geq \langle W \rangle - \frac{\beta}{2} (\langle W^2 \rangle - \langle W \rangle^2). \quad (18)$$

However, in this case the bias can be corrected by using the unbiased estimator for the variance.³⁸ Namely, if we use

$$\Psi_M \equiv \frac{1}{M} \sum_{i=1}^M W_i - \frac{\beta}{2} \frac{M}{M-1} \left[\frac{1}{M} \sum_{i=1}^M W_i^2 - \left(\frac{1}{M} \sum_{i=1}^M W_i \right)^2 \right] \quad (19)$$

to estimate the second order cumulant expansion, the resulting estimate is unbiased:

$$\langle \Psi_M \rangle = \langle W \rangle - \frac{\beta}{2} (\langle W^2 \rangle - \langle W \rangle^2). \quad (20)$$

The effect of this finite-sampling correction is shown in Fig. 6 for two different pulling speeds, 10 and 100 \AA/ns . Although not to a large degree, the finite-sampling correction improves the resulting PMF. The unbiased esti-

mate [Eq. (19)] is hence recommended, especially when the number of trajectories at hand is small.

3. Work fluctuation and the accuracy of the calculated free energy

The fluctuation of work is often used as a measure of the applicability of Jarzynski's equality. Only when the fluctuation of work is comparable to the temperature, Jarzynski's equality is considered practically applicable.^{5,19,21} Thus, it is worth comparing the fluctuation of work and the accuracy of the calculated free energy in the present example. Since the accuracy of the calculated free energy generally decreases with pulling distance, we report the standard deviation of the total

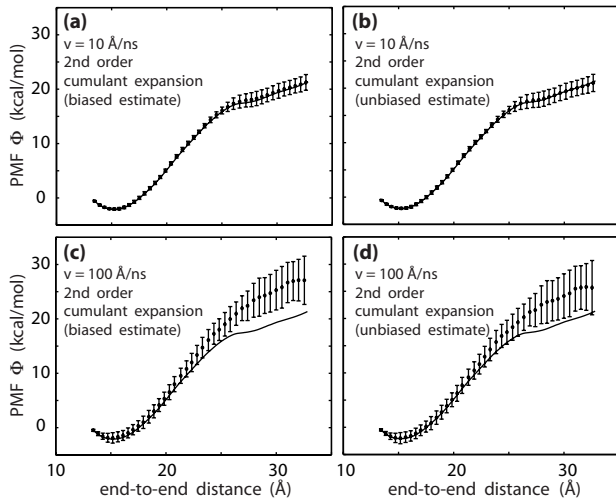


FIG. 6: Finite-sampling correction. PMFs calculated through the biased estimate [Eq. (18)] and the unbiased estimate [Eq. (19)] are compared. The solid lines show the exact free energy calculated from the reversible pulling.

work W_{total} and the accuracy of the estimated free energy difference $\Delta\Phi_{\text{total}}^{\text{est}}$ between the initial and the final configuration. For $v = 10 \text{ \AA/ns}$, the standard deviation of the total work, $\sqrt{\langle W_{\text{total}}^2 \rangle - \langle W_{\text{total}} \rangle^2}$, is about 1.9 kcal/mol ($3.1 k_B T$). The mean error $\sqrt{\langle (\Delta\Phi_{\text{total}}^{\text{est}} - \Delta\Phi_{\text{total}})^2 \rangle_{\text{block}}}$ calculated through a block average is about 1.6 kcal/mol, which corresponds to 7.6% of the actual value ($\Delta\Phi_{\text{total}} = 21.4 \text{ kcal/mol}$). For $v = 100 \text{ \AA/ns}$, the standard deviation of the total work is 4.3 kcal/mol ($7.1 k_B T$) and the mean error is 6.7 kcal/mol, corresponding to 31%. These errors indicate the accuracy of the free energy calculated from 10 trajectories.

4. Choice of the force constant

The proper choice of the force constant k for the guiding potential [Eq. (4)] is important. The stiff-spring approximation, i.e. Eq. (10), is valid only if the force constant is sufficiently large that the reaction coordinate closely follows the constraint position. As shown in Appendix, the chosen force constant, $k = 500 \text{ pN/\AA}$, is large enough to ensure the validity of the stiff-spring approximation. But, following Ref. 13 we ask if one can choose any arbitrarily large force constant? In order to address this question, we repeated the pulling simulation with significantly larger force constant, 35000 pN/\AA , which is in the range of typical force constants for covalent bonds. In Fig. 7, the resulting PMF is compared to that obtained with the original force constant. Although there is no essential difference between the two results, the PMF calculated with the larger force constant shows larger fluctuations, which is likely due to the large fluctuation of the external force that scales as $\sqrt{k k_B T}$.¹³ Therefore, it is recommended that the force constant be chosen large

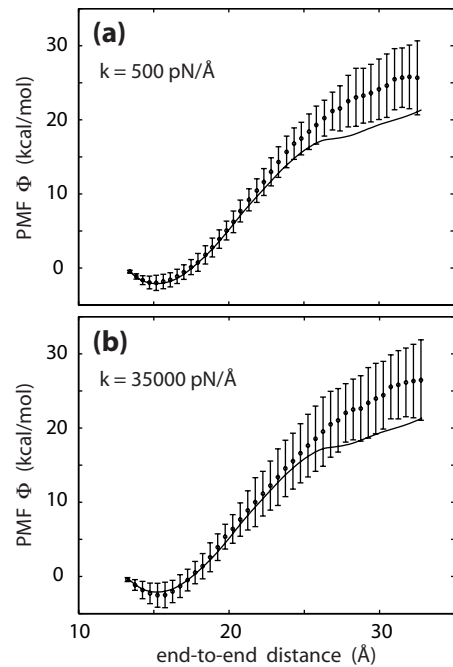


FIG. 7: PMF calculated by using two different force constants (500 and 35000 pN/Å) for the same pulling speed (100 Å/ns). The unbiased formula for the second order cumulant expansion, Eq. 19, was used.

enough to ensure small deviation of the reaction coordinate from the constraint position, but not much larger than that.

C. Comparison with umbrella sampling

Umbrella sampling³ is a traditional method of PMF calculation. In order to compare the efficiencies of the present nonequilibrium thermodynamic integration method and umbrella sampling, we performed a PMF calculation for our system based on umbrella sampling. Ten harmonic biasing potentials, $(A/2)(\xi - \xi_0)^2$ with $A = 70 \text{ pN/\AA}$ and $\xi_0 = 13.4, 16.1, 18.5, 20.4, 22.5, 24.8, 26.4, 28.5, 30.5, 33.0 \text{ \AA}$, were used to sample the end-to-end distance ξ . The histograms obtained from simulations with biasing potentials at different locations were combined with the weighted histogram analysis method.³⁹

We compare the two methods based on an equal amount of simulation time. The result shown in Fig. 8c was obtained with the same simulation time as in the pulling simulation at the speed of 10 \AA/ns . Thus, Fig. 8c can be directly compared to Fig. 6b. Likewise, Fig. 8d can be directly compared to Fig. 6d. As in the pulling simulations, averages and fluctuations of PMF were calculated through a block analysis of 10 blocks. As can be seen from these figures, it is rather hard to tell which method is better. The fluctuation over blocks is smaller in the umbrella sampling method, but the deviation from

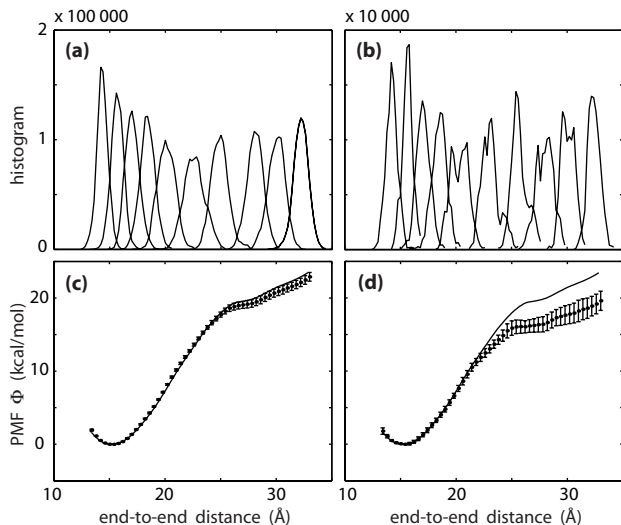


FIG. 8: PMF calculated from umbrella sampling simulations. (a) and (c): 2 ns simulation for each histogram; 10 histograms for each block; 10 blocks in total. (b) and (d): 0.2 ns simulation for each histogram; 10 histograms for each block; 10 blocks in total. (a) and (b) show histograms in one block out of the ten blocks. In (c) and (d), the error bars indicate the standard deviation over the blocks, and the exact PMF is plotted as a solid line. The minimum at $\xi = 15.2 \text{ \AA}$ was chosen as a reference point for calculating block averages.

the exact PMF is more noticeable. Hummer²² also compared nonequilibrium thermodynamic integration and umbrella sampling in a calculation of PMF for the separation of two methane molecules in water, and concluded that the efficiencies of the two methods are comparable.

In general, the analysis involved in the present method is simpler than that involved in umbrella sampling in which one needs to solve coupled nonlinear equations for the weighted histogram analysis method.¹ In addition, the present method has the advantage of uniform sampling of a reaction coordinate. Whereas in umbrella sampling a reaction coordinate is sampled nonuniformly proportional to the Boltzmann weight, in the present method a reaction coordinate follows a guiding potential that moves with a constant velocity, and hence is sampled almost uniformly (computing time is uniformly distributed over the given region of the reaction coordinate). This is particularly beneficial when a PMF contains narrow barrier regions as in Ref. 15. In such cases, a successful application of umbrella sampling depends on

an optimal choice of biasing potentials, whereas nonequilibrium thermodynamic integration seems more robust.¹

IV. CONCLUSION

We have presented a method of free energy calculation based on Jarzynski's equality and the stiff-spring approximation, and applied it to an SMD simulation of the helix-coil transition of deca-alanine in vacuum. We find that when only a limited number (about ten) of trajectories of irreversible processes (100~1000 times faster than the reversible regime) are available, the second order cumulant expansion yields the most accurate estimate, which can be further improved by using the unbiased estimate. This conclusion only applies to the case of relatively small sampling sizes. As the sampling size grows, the exponential average will eventually become the most accurate.²⁰ We have compared the present method and umbrella sampling and found that the efficiencies of the two methods are comparable.

Acknowledgments

We are grateful to the referee whose constructive comment lead us to the analysis in Appendix. This work was supported by National Institutes of Health grants PHS-5-P41-RR05969 and R01-GM60946.

APPENDIX: THE STIFF-SPRING APPROXIMATION

Here we systematically derive the stiff-spring approximation formula, Eq. (10), including correction terms. As shown in Eq. (9), the exact relation between the free energy F and the PMF Φ is

$$\exp[-\beta F(\lambda)] = \int d\xi \exp \left[-\frac{\beta k}{2}(\xi - \lambda)^2 - \beta \Phi(\xi) \right]. \quad (\text{A.1})$$

When k is large, most of the contribution to the integral comes from the region around $\xi = \lambda$. Thus, a series expansion about $k = \infty$ can be obtained by taking the Taylor series of $\exp[-\beta \Phi(\xi)]$ about λ followed by respective integrations:

$$\begin{aligned} \exp[-\beta F(\lambda)] &= \int d\xi \exp \left[-\frac{\beta k}{2}(\xi - \lambda)^2 \right] \exp[-\beta \Phi(\lambda)] \\ &\quad \times \left\{ 1 - \beta \Phi'(\lambda)(\xi - \lambda) - \frac{\beta}{2} [\Phi''(\lambda) - \beta \Phi'(\lambda)^2](\xi - \lambda)^2 + \dots \right\} \end{aligned}$$

$$= \exp[-\beta\Phi(\lambda)] \sqrt{\frac{2\pi}{\beta k}} \left\{ 1 - \frac{1}{2k} [\Phi''(\lambda) - \beta\Phi'(\lambda)^2] + O(1/k^2) \right\}. \quad (\text{A.2})$$

Upon taking the logarithm and dropping the terms independent of λ , we find

$$F(\lambda) = \Phi(\lambda) - \frac{1}{2k}\Phi'(\lambda)^2 + \frac{1}{2\beta k}\Phi''(\lambda) + O(1/k^2). \quad (\text{A.3})$$

This series can be inverted to yield a formula for $\Phi(\lambda)$:

$$\Phi(\lambda) = F(\lambda) + \frac{1}{2k}F'(\lambda)^2 - \frac{1}{2\beta k}F''(\lambda) + O(1/k^2), \quad (\text{A.4})$$

which shows the first order correction to the stiff-spring approximation. If desired, higher order corrections can

be obtained in a similar way.

The correction terms can be estimated from $F(\lambda)$ obtained from simulations. In the case of the present example (for $k = 500$ pN/Å), the magnitude of the correction is less than 0.5 kcal/mol which is indeed small compared to the overall scale of the PMF. The validity of the stiff-spring approximation is therefore verified.

-
- ¹ D. Frenkel and B. Smit, *Understanding Molecular Simulation: From Algorithms to Applications* (Academic Press, San Diego, 2002), 2nd ed.
- ² J. G. Kirkwood, *J. Chem. Phys.* **3**, 300 (1935).
- ³ G. M. Torrie and J. P. Valleau, *Chem. Phys. Lett.* **28**, 578 (1974).
- ⁴ T. Simonson, in *Computational Biochemistry and Biophysics*, edited by O. M. Becker, A. D. MacKerell, Jr, B. Roux, and M. Watanabe (Marcel Dekker, New York, 2001), pp. 169–197.
- ⁵ C. Jarzynski, *Phys. Rev. Lett.* **78**, 2690 (1997).
- ⁶ B. Isralewitz, J. Baudry, J. Gullingsrud, D. Kosztin, and K. Schulten, *Journal of Molecular Graphics and Modeling* **19**, 13 (2001).
- ⁷ B. Isralewitz, M. Gao, and K. Schulten, *Curr. Op. Struct. Biol.* **11**, 224 (2001).
- ⁸ A. Krammer, H. Lu, B. Isralewitz, K. Schulten, and V. Vogel, *Proc. Nat. Acad. Sci. USA* **96**, 1351 (1999).
- ⁹ M. Gao, M. Wilmanns, and K. Schulten, *Biophys. J.* **83**, 3435 (2002).
- ¹⁰ M. Gao, D. Craig, V. Vogel, and K. Schulten, *J. Mol. Biol.* **323**, 939 (2002).
- ¹¹ S. Izrailev, S. Stepaniants, M. Balsera, Y. Oono, and K. Schulten, *Biophys. J.* **72**, 1568 (1997).
- ¹² M. V. Bayas, K. Schulten, and D. Leckband, *Biophys. J.* **84**, 2223 (2003).
- ¹³ M. Balsera, S. Stepaniants, S. Izrailev, Y. Oono, and K. Schulten, *Biophys. J.* **73**, 1281 (1997).
- ¹⁴ J. Gullingsrud, R. Braun, and K. Schulten, *J. Comp. Phys.* **151**, 190 (1999).
- ¹⁵ M. Ø. Jensen, S. Park, E. Tajkhorshid, and K. Schulten, *Proc. Nat. Acad. Sci. USA* **99**, 6731 (2002).
- ¹⁶ R. Amaro, E. Tajkhorshid, and Z. Luthey-Schulten, *Proc. Nat. Acad. Sci. USA* (in press).
- ¹⁷ H. B. Callen, *Thermodynamics and an Introduction to Thermostatistics* (John Wiley & Sons, New York, 1985), 2nd ed.
- ¹⁸ C. Jarzynski, *Phys. Rev. E* **56**, 5018 (1997).
- ¹⁹ J. Liphardt, S. Dumont, S. B. Smith, I. Tinoco Jr., and C. Bustamante, *Science* **296**, 1832 (2002).
- ²⁰ D. A. Hendrix and C. Jarzynski, *J. Chem. Phys.* **114**, 5974 (2001).
- ²¹ G. Hummer and A. Szabo, *Proc. Nat. Acad. Sci. USA* **98**, 3658 (2001).
- ²² G. Hummer, *J. Chem. Phys.* **114**, 7330 (2001).
- ²³ D. M. Zuckerman and T. B. Woolf, *Chem. Phys. Lett.* **351**, 445 (2002).
- ²⁴ D. M. Zuckerman and T. B. Woolf, *Phys. Rev. Lett.* **89**, 180602 (2002).
- ²⁵ S. Izrailev, S. Stepaniants, B. Isralewitz, D. Kosztin, H. Lu, F. Molnar, W. Wriggers, and K. Schulten, in *Computational Molecular Dynamics: Challenges, Methods, Ideas*, edited by P. Deuffhard, J. Hermans, B. Leimkuhler, A. E. Mark, S. Reich, and R. D. Skeel (Springer-Verlag, Berlin, 1998), vol. 4 of *Lecture Notes in Computational Science and Engineering*, pp. 39–65.
- ²⁶ G. Binnig, C. F. Quate, and C. Gerber, *Phys. Rev. Lett.* **56**, 930 (1986).
- ²⁷ S. Nosé, *J. Chem. Phys.* **81**, 511 (1984).
- ²⁸ W. G. Hoover, *Phys. Rev. A* **31**, 1695 (1985).
- ²⁹ J. Marcinkiewicz, *Math. Z* **44**, 612 (1939).
- ³⁰ R. H. Wood, W. C. F. Mühlbauer, and P. T. Thompson, *J. Phys. Chem.* **95**, 6670 (1991).
- ³¹ J. Hermans, *J. Phys. Chem.* **95**, 9029 (1991).
- ³² W. Humphrey, A. Dalke, and K. Schulten, *J. Mol. Graphics* **14**, 33 (1996).
- ³³ Y. Levy, J. Jortner, and O. M. Becker, *Proc. Nat. Acad. Sci. USA* **98**, 2188 (2001).
- ³⁴ Rotation around the z-axis was not removed. Since we are interested in relative free energies, the removal of irrelevant degrees of freedom does not affect the result. It merely makes the analysis of trajectories easier.
- ³⁵ L. Kalé, R. Skeel, M. Bhandarkar, R. Brunner, A. Gursoy, N. Krawetz, J. Phillips, A. Shinzaki, K. Varadarajan, and K. Schulten, *J. Comp. Phys.* **151**, 283 (1999).
- ³⁶ A. D. MacKerell Jr, D. Bashford, M. Bellott, R. L. Dunbrack Jr., J. Evanseck, M. J. Field, S. Fischer, J. Gao, H. Guo, S. Ha, et al., *J. Phys. Chem. B* **102**, 3586 (1998).
- ³⁷ If the molecule is stretched further, the entropy will decrease again since the available configuration space will eventually reduce.
- ³⁸ J. F. Kenney and E. S. Keeping, *Mathematics of Statistics*

(Van Nostrand, Princeton, 1951), 2nd ed.
³⁹ A. M. Ferrenberg and R. H. Swendsen, Phys. Rev. Lett.

63, 1195 (1989).